

See discussions, stats, and author profiles for this publication at: <https://www.researchgate.net/publication/51466443>

Single-Monomer Formulation of Polymerized Polyethylene Glycol Diacrylate as a Nonadsorptive Material for Microfluidics

ARTICLE *in* ANALYTICAL CHEMISTRY · AUGUST 2011

Impact Factor: 5.64 · DOI: 10.1021/ac201539h · Source: PubMed

CITATIONS

17

READS

34

4 AUTHORS, INCLUDING:



Jayson Pagaduan

Johns Hopkins University

9 PUBLICATIONS 59 CITATIONS

SEE PROFILE



Greg Nordin

Brigham Young University - Provo Main Cam...

131 PUBLICATIONS 1,335 CITATIONS

SEE PROFILE

Published in final edited form as:

Anal Chem. 2011 August 15; 83(16): 6418–6425. doi:10.1021/ac201539h.

Single-Monomer Formulation of Polymerized Polyethylene Glycol Diacrylate as a Nonadsorptive Material for Microfluidics

Chad I. Rogers[†], Jayson V. Pagaduan[†], Gregory P. Nordin[‡], and Adam T. Woolley^{†,*}

[†]Department of Chemistry and Biochemistry, Brigham Young University, Provo, UT 84602

[‡]Department of Electrical and Computer Engineering, Brigham Young University, Provo, UT 84602

Abstract

Nonspecific adsorption in microfluidic systems can deplete target molecules in solution and prevent analytes, especially those at low concentrations, from reaching the detector. Polydimethylsiloxane (PDMS) is a widely used material for microfluidics, but is prone to nonspecific adsorption, necessitating complex chemical modification processes to address this issue. An alternative material to PDMS that does not require subsequent chemical modification is presented here. Poly(ethylene glycol) diacrylate (PEGDA) mixed with photoinitiator forms on exposure to UV radiation a polymer with inherent resistance to nonspecific adsorption. Optimization of the polymerized PEGDA (poly-PEGDA) formula imbues this material with some of the same properties, including optical clarity, water stability, and low background fluorescence, that make PDMS so popular. Poly-PEGDA demonstrates less nonspecific adsorption than PDMS over a range of concentrations of flowing fluorescently tagged bovine serum albumin solutions, and poly-PEGDA has greater resistance to permeation by small hydrophobic molecules than PDMS. Poly-PEGDA also exhibits long-term (hour scale) resistance to nonspecific adsorption compared to PDMS when exposed to a low (1 $\mu\text{g/mL}$) concentration of a model adsorptive protein. Electrophoretic separations of amino acids and proteins resulted in symmetrical peaks and theoretical plate counts as high as $4 \times 10^5/\text{m}$. Poly-PEGDA, which displays resistance to nonspecific adsorption, could have broad use in small volume analysis and biomedical research.

Introduction

The field of microfluidics has gained increasing research focus for small volume analysis over the last twenty years.^{1–4} Ideally, microfluidic devices must be small and inexpensive, have rapid analysis times, and not require extensive training to use. As specimen sizes get smaller, microfluidics provide a means for reagent control and delivery, improved mass transport, and more efficient sample use in small spaces. Recent examples of the power of microfluidic systems can be found in cell-based assays,^{5, 6} droplet microfluidics,^{7–10} and chemical analysis.^{11–13} Goral et al.¹⁴ used polydimethylsiloxane (PDMS) in a perfusion-based microsystem to mimic *in vivo* conditions for hepatocytes without the need for special matrices or coagulants. Shi et al.¹⁵ utilized a droplet microfluidic system made from PDMS to immobilize an array of nematodes and test the effects of varying doses of neurotoxins. Yang et al.^{16, 17} recently showed that poly(methyl methacrylate) devices having

*To whom correspondence should be addressed. Department of Chemistry and Biochemistry, Brigham Young University, Provo, UT 84602. atw@byu.edu.

Associated Content

Supporting Information. Additional figures and tables as noted in text. This material is available free of charge via the Internet at <http://pubs.acs.org>.

photopolymerized affinity columns could be used to selectively purify and quantitate cancer-related biomarkers from a complex sample such as blood serum. These examples demonstrate the great potential of microfluidics in biomedical research and point-of-care clinical analysis.

Biological samples pose a particular problem of interest for microfluidic systems. However, PDMS, a popular material in these microfluidic systems, is prone to nonspecific adsorption and fouling.^{18, 19} Because biological samples may be limited to very small quantities, some or all of the analytes of interest could be lost to an adsorptive surface, instead of being detected. Although many methods have attempted to address this important issue by modifying the PDMS itself,^{20–24} an increasingly attractive alternative is to find a replacement material for PDMS, which retains the ability to be patterned and formed easily, but does not suffer from severe surface fouling.

Most current research in microfluidics uses static or dynamic surface changes to reduce adsorption to the device material. In PDMS, plasma oxidation has been shown to increase the hydrophilicity of the surface, but the effect is only temporary (lasting hours) due to low molecular weight oligomers that are present in the bulk of the PDMS and return slowly to the surface;^{25, 26} this process can be slowed if the oxidized PDMS is rapidly transferred to water.²⁷ Solution-phase reactions can be used to functionalize oxidized PDMS surfaces with perfluorosilanes²⁸ or polyethylene glycol silanes.²⁹ Dynamic surface modification methods are by definition temporary coatings that need to be replenished frequently.

Alternative materials to PDMS have been developed in the last ten years, but have yet to gain significant traction. Perfluoropolymers like perfluoropolyether (PFPE)^{30, 31} provide inherent resistance to nonspecific adsorption and have been used instead of PDMS as microfluidic supports, but bonding separate layers can be problematic. Thermoset polyester microfluidic devices³² use similar soft photolithography methods to PDMS for fabrication; however, atom-transfer radical polymerization was needed to passivate surfaces before protein separations.³³ A mildly hydrophilic polymer, polyethylene glycol (PEG), is known for its resistance to nonspecific binding.³⁴ Integrating PEG directly into PDMS has been attempted, but the optical clarity of the resulting polymer is greatly reduced.³⁵ Incorporating PEG into an acrylate plastic creates an optically clear, UV curable polymer that can be formed using soft lithography techniques.³⁶ Repeating PEG subunits in the bulk of the polymer provide an inherent way to reduce nonspecific binding in fluidic pathways without further chemical modification or replenishment. Kim et al.³⁷ demonstrated that either PEG diacrylate (PEGDA) or PEG dimethacrylate (PEGDMA), when mixed with photoinitiator, could be cured quickly via UV exposure and form stable channel features as small as 50 nm. Undercured individual layers were bonded after they were placed together and fully cured. Poly-PEGDMA was shown to offer lower nonspecific protein and cell adhesion than either PDMS or PEG-silanized PDMS, but no adsorption studies on poly-PEGDA were done. Furthermore, analytical separations were not demonstrated in either poly-PEGDMA or poly-PEGDA devices. Liu et al.³⁶ polymerized a multicomponent mixture of acrylate monomers, some of which included PEG groups, and demonstrated this material's potential as a microfluidic substrate for capillary electrophoresis. PEG methyl ether methacrylate (PEGMEMA) was included in the formulation to extend the UV exposure time, but methyl methacrylate (MMA), a more hydrophobic monomer that lacks a PEG moiety and raises nonspecific adsorption concerns, was required to regain rigidity in the resulting polymer.

This paper describes the development of polymerized PEGDA (poly-PEGDA) as a nonadsorptive alternative microfluidics material to PDMS. We demonstrate that varying the composition of monomer and changing the photoinitiator concentration in poly-PEGDA formulas can affect the water stability, bond strength (burst pressure), and optical clarity of

the resulting polymer. Poly-PEGDA made with a low photoinitiator concentration and three ethylene glycol repeats (258 Da monomer) had the best combination of these properties, and was further optimized to have background fluorescence comparable to PDMS. Importantly, poly-PEGDA demonstrated better resistance than PDMS to permeation of small hydrophobic molecules. Innate resistance to protein adsorption in uncoated and unmodified poly-PEGDA was demonstrated by flowing increasing protein concentrations through PDMS and poly-PEGDA microchannels to compare nonspecific adsorption over a six order-of-magnitude concentration range. Furthermore, a low concentration (1 $\mu\text{g/mL}$) of fluorescently labeled bovine serum albumin flowed through microchannels was utilized to illustrate the difference in nonspecific adsorption between PDMS and poly-PEGDA over time. Poly-PEGDA exhibited a stable fluorescence signal while the PDMS fluorescence signal increased by over threefold in an hour's time. Finally, microchip electrophoresis experiments demonstrated that poly-PEGDA sustains stable electroosmotic flow and enables quality separations.

Experimental

Materials

Fluorescein isothiocyanate labeled bovine serum albumin (FITC-BSA), PEGDA (M.W. 258), PEGMEMA (M.W. 1100), MMA (99%), 2,2'-dimethoxy-2-phenylacetophenone (DMPA), Rhodamine B base (97%), DL-tryptophan (99%), dimethyl sulfoxide (DMSO, 99.7%), porcine thyroglobulin, and β -lactoglobulin A were purchased from Sigma-Aldrich (Milwaukee, WI). L-lysine HCl was obtained from United States Biochemical Corporation (Cleveland, OH) and FITC was acquired from Invitrogen (Carlsbad, CA). Anhydrous granular sodium sulfate (99.2%) and dichloromethane (99.5%) were purchased from Mallinckrodt (Phillipsburg, NJ). Omnipur 10 \times phosphate buffer solution was purchased from EMD Chemicals (Gibbstown, NJ) and diluted to 1 \times with deionized (DI) water (18.2 M Ω). An aqueous saturated solution of sodium carbonate was made from powdered anhydrous sodium carbonate (99.5%, EMD Chemicals) and DI water. Boric acid (99.5%) obtained from EM Science (Darmstadt, Germany), sodium tetraborate decahydrate (99.5%) acquired from Sigma-Aldrich, and DI water were used to make 25 mM borate buffer (pH 9.3). Rhodamine B base was diluted in borate buffer to create a 10 μM solution. A mixture of sodium carbonate (99.5%) purchased from EMD Chemicals, sodium bicarbonate (99.7%) obtained from EM Science, and DI water was used to make carbonate buffers at pH 9.3 and pH 10.0. SU8-2025, SU8-2015 and SU8 developer were purchased from Microchem (Newton, MA). PDMS Sylgard 184 base and curing agent were obtained from Dow Corning (Midland, MI).

PDMS Fabrication Summary

PDMS microfabrication is well known in the literature^{38–40} and is only summarized briefly here. A two-layer flow channel is made, starting with fabrication of the upper PDMS layer by plasma cleaning of a silicon wafer at 250 W for 3 min using a Planar Etch II system (Technics, San Jose, CA). SU8-2025 was spun onto the cleaned wafer at 900 rpm to the desired thickness of 60–80 μm . A patterned chrome-coated glass mask was used to define the desired design into the photoresist. After UV exposure for 50 s, the resist was developed in SU8 developer, leaving raised rectangular-shaped features. The SU8 pattern formed a negative mold for the PDMS. A 4:1 ratio of PDMS to curing agent was mixed, degassed, poured over the SU8 mold and allowed to cure at 80 $^{\circ}\text{C}$ for 45 min. The \sim 2-mm-thick cured PDMS was removed, cut to size using a razor, and input and output holes were punched using a 21 gauge needle. A 3.5" diameter glass wafer was plasma cleaned as before. A 3:1 ratio of PDMS to curing agent was mixed, degassed, and spun onto the wafer using a Laurell Spinner (WS-400A-6NPP-LITE, North Wales, PA) at 2000 rpm for 60 s. This thin PDMS

was allowed to cure at 80°C for 45 min. The molded upper layer was stamped in curing agent and placed onto the lower layer, and the combined structure was heated to 80°C for 1 hr to bond the two layers together.

Poly-PEGDA Fabrication Summary

The fabrication process of a poly-PEGDA flow channel is shown in Figure 1. PEGDA is a liquid which requires a mold to form structures via polymerization; the chemical structures of the PEGDA monomer and poly-PEGDA are depicted in Figure A in the Supporting Information online. The flow channel mold was made by patterning SU8-2025 on a surface (Figure 1A-1, 2). A PDMS-coated glass piece and poly-PEGDA spacers were used to define the polymerization region for the upper layer (Figure 1A-3). PDMS was coated onto the glass wafer to facilitate the removal of the cover plate. A Karl Suss Aligner was used to expose the wafer to 10 mW/cm² UV light. Exposure time varied depending upon the polymer thickness and formula. Once polymerized, the poly-PEGDA was easily removed from the mold (Figure 1A-4), cut into individual dies, and holes were formed into the poly-PEGDA using a CO₂ laser cutter (VersaLASER VLS 2.30, Scottsdale, AZ). Although other methods, such as using PDMS cylinders in the polymer cast, can be used to form reservoir holes,³⁶ laser cutting provides reproducibility and patterning flexibility for different designs. The poly-PEGDA substrates were cleaned with isopropyl alcohol to remove any residue or debris left on the surface. A second, unpatterned poly-PEGDA layer was created with a similar setup to Figure 1A-3 but using glass slides and poly-PEGDA spacers to form the mold (Figures 1A-6, 7).

Excess liquid at the surface of the bottom layer was removed. The poly-PEGDA layers were intentionally undercured to help bind the two layers together subsequently; if either layer was significantly overcured, success in irreversible bonding of the two decreased. The top layer was placed onto the bottom layer and any bubbles that formed at the interface were extruded by gently applying pressure. A second exposure to UV light completed the curing and bonding process (Figure 1A-8). Nanoports (Upchurch Scientific, Oak Harbor, WA) were attached to the finished poly-PEGDA device to allow interfacing with tubing and a syringe pump (Figure 1B). The completed device was then taped onto a glass slide (Figure 1A-9).

Formula Optimization

A series of different poly-PEGDA formulations was tested for optical clarity, water stability, and polymerization. The variations evaluated were as follows: the molecular weight of PEGDA (258 vs. 575 Da), 0.05% vs. 3% DMPA photoinitiator, PEGDA with different amounts of additives (PEGMEMA and MMA) vs. PEGDA-only, and polymerization for 10 s vs. 25 s (see Supporting Information online, Tables S1–S3). Each variant was rated for clarity on a 0–2 scale and polymerization on a 0–5 scale. The polymer samples were then completely immersed in water for 16 hrs to test for stability in an aqueous environment.

To remove any impurities from PEGDA that might contribute to background fluorescence, we used a purification method reported previously by Liu et al.³⁶ Briefly, 50 mL of PEGDA monomer was rinsed with three 30 mL aliquots of a saturated solution of Na₂CO₃. The PEGDA was then rinsed with three 50 mL aliquots of dichloromethane. Residual water was removed with granular sodium sulfate, and a rotovap was used to remove the dichloromethane.

Burst Pressure Testing

A completed poly-PEGDA device was attached to tubing and a syringe pump. DI water was pumped through the channel to displace the air. Once the channel was clear of bubbles, a

piece of PDMS was placed over the exit and held in place using a clamp (Figure 2A). A Honeywell pressure sensor (24PCFFA6G) was attached in-line using the same setup as Satyanarayana et al.⁴¹ Pressure sensor data as fluid was pumped into the channel was recorded as a function of time using LabView.

Bulk Fluorescence Comparison

To test bulk fluorescence properties, 700- μm -thick layers were formed of PDMS, poly-PEGDA made with 1% DMPA, and poly-PEGDA made with filtered monomer and 1% DMPA. Regions illuminated by a Reliant 150M 488 nm laser (Laser Physics, West Jordan, UT) expanded to a ~ 1.4 -mm-diameter diffuse beam were imaged using a CoolSNAPHQ CCD (Photometrics, Tucson, AZ). The power of the laser at the detection point was 1 mW. After initial images the devices were exposed to ~ 3.5 mW at the detection point for thirty minutes to survey for any photobleaching once the power was returned to 1 mW and additional fluorescence images were taken.

Rhodamine B Comparison

Roman et al.⁴² demonstrated that hydrophobic molecules such as rhodamine B can readily diffuse into PDMS. We used a similar method to compare the diffusion of rhodamine B into poly-PEGDA and PDMS. A 50 μm wide, ~ 20 μm tall, and 3.0 cm long feature made from patterned SU8-2015 was used to cast channels in both materials. Fluorescence images using the same laser/CCD setup as above were obtained for the channels under flow (0.2 $\mu\text{L}/\text{min}$) of borate buffer (0 min) and 10 μM rhodamine B at several time intervals up to 4 hr. The laser was blocked between measurements to avoid photobleaching.

Fluorescence Comparison

PDMS and poly-PEGDA two-layer devices, each having a flow channel, were used to compare nonspecific binding on channel surfaces. Laser induced fluorescence (LIF) at 488 nm as described above was used to detect nonspecific adsorption of FITC-BSA. Background signal for the polymer in each device was photobleached by raising the laser power from 1 to 3.5 mW at the detection point for 15 min.

A series of exposures to increasing concentrations of FITC-BSA followed by buffer rinses was used to compare nonspecific binding for PDMS and poly-PEGDA. Initially, $1\times$ PBS solution was rinsed through the flow channel at 110 $\mu\text{L}/\text{min}$ rate for 3 min. The flow was reduced to 10 $\mu\text{L}/\text{min}$ and allowed to flow for 1 min before a fluorescence image was taken. A sample of 1 ng/mL FITC-BSA was introduced in the same fashion and allowed to sit in the channel with no flow for 5 min. An image was taken after resuming flow for 1 min at 10 $\mu\text{L}/\text{min}$. The laser was blocked except during fluorescence measurement to avoid photobleaching of surface-adsorbed molecules. PBS was then used to rinse the channel as before, and another image was taken with buffer only in the channel. These steps were repeated for FITC-BSA concentrations increasing from 3 ng/mL to 1 mg/mL. The fluorescence images from the CCD were analyzed using ImageJ 1.43u. In all cases, background images were captured with buffer flowing in the channel at 10 $\mu\text{L}/\text{min}$, and the resulting background signal was subtracted from the sample fluorescent images.

Time Comparison

A low concentration of a model adsorptive species (FITC-BSA) flowed slowly through a micro-channel enables the determination of the time dependence of nonspecific binding for a substrate. The flow rate was set such that diffusional transport would allow FITC-BSA throughout the channel to interact with the surface prior to the detection location. The equation for diffusion in one dimension is given by

$$x = \sqrt{4Dt} \quad (1)$$

where x is distance, D is the diffusion coefficient, and t is time.⁴³ A value of $D = 6 \times 10^{-7} \text{ cm}^2/\text{s}$ was used for FITC-BSA.⁴⁴ Rearranging Equation 1 to solve for t gives the time for a molecule to diffuse across a distance x . In our channel geometry, $\sim 27 \text{ s}$ is required for a FITC-BSA molecule to diffuse $80 \text{ }\mu\text{m}$ (top to bottom surface), and just $\sim 7 \text{ s}$ are needed to travel $40 \text{ }\mu\text{m}$ (mid-channel to wall). FITC-BSA in solution flowing at $0.2 \text{ }\mu\text{L}/\text{min}$ to our shortest distance to detection (0.2 cm) would take $\sim 14 \text{ s}$ to arrive, thus allowing adequate time for any given FITC-BSA molecule to come into contact with the channel surface prior to the detection point.

The flow channel and detection setup were the same as described previously. The channel was rinsed with PBS for 10 min at $100 \text{ }\mu\text{L}/\text{min}$ to remove any bubbles or debris. After rinsing, an air bubble was introduced into the channel before a $1 \text{ }\mu\text{g}/\text{mL}$ solution of FITC-BSA (to signal when the sample had entered the channel). Data acquisition started when the bubble was visible in the channel but before the fluorescent sample had entered the detection zone. Images were taken every minute for poly-PEGDA, and every minute for PDMS for the first 35 min, with images taken every five or ten minutes thereafter.

Microchip Electrophoresis

Lysine and tryptophan at $1 \text{ mg}/\text{mL}$ in carbonate buffer (pH 9.3) were labeled with $4 \text{ mg}/\text{mL}$ FITC in DMSO by mixing $25 \text{ }\mu\text{L}$ of FITC solution with $75 \text{ }\mu\text{L}$ of amino acid solution and reacting at room temperature for 24 hr.¹⁶ β -lactoglobulin A ($2 \text{ mg}/\text{mL}$) was labeled with FITC by mixing $5 \text{ }\mu\text{L}$ of FITC solution with $100 \text{ }\mu\text{L}$ of protein solution, while thyroglobulin was labeled by mixing $10 \text{ }\mu\text{L}$ of FITC solution with $100 \text{ }\mu\text{L}$ of $2 \text{ mg}/\text{mL}$ thyroglobulin. Protein solutions were then filtered to remove excess FITC using a 3 kDa Amicon Ultra filter (Billerica, MA). Protein concentrations were quantified using a Nanodrop ND-1000 spectrophotometer (Wilmington, DE).

The offset-T design electrophoresis microchip⁴⁵ was fabricated in poly-PEGDA, as described above for the Rhodamine B test devices. The injection arms were 0.5 cm long, and the separation channel was 3.0 cm from the intersection to the end reservoir. The channels were $50 \text{ }\mu\text{m}$ wide and $18 \text{ }\mu\text{m}$ tall. Pinched injection times of 20 s for amino acids and 30 s for proteins were used to introduce the analytes into the separation channel. The amino acid separation used -850 V across the injection pathway, -2000 V along the separation channel, and pH 9.3 carbonate buffer. Protein analysis was done using -900 V for injection and -2000 V for separation with pH 10.0 carbonate buffer. Fluorescence was collected at a separation distance of 2.5 cm using a point detection system described previously.⁴⁵

Results and Discussion

Formula Optimization

The polymer formulation is critical to achieving desired device properties. If a higher molecular weight of PEGDA (i.e., 575 or 700 Da) is used, the resulting polymer is susceptible to swelling, and eventual buckling and cracking when exposed to water, typically within as little as 10 min of submersion (similar to results from Kim et al.³⁷) The concentration of DMPA affected the rate of polymerization: higher concentrations required shorter UV exposure times but generated heat which resulted in cracking of the polymer material. Addition of PEGMEMA increased the UV exposure time but required the use of MMA in higher concentrations for structural stability. By comparing a series of formulations including PEGDA-only, we determined an optimal formula for making thin ($\sim 350 \text{ }\mu\text{m}$)

layers while maintaining optical clarity and water stability. Scanning electron microscopy images detail channel features in poly-PEGDA (see Supporting Information online, Figure B).

Poly-PEGDA made from a low molecular weight PEGDA (258 Da) and having 0.0015–1.0% DMPA photoinitiator was found to be the most stable in water while still having good optical clarity (see Supporting Information online, Figure C). Although three other polymer formulations that also contained PEGMEMA and MMA in addition to PEGDA survived submersion for more than 16 hours, the PEGDA-only formulas were simpler to prepare and had some mechanical flexibility (see Supporting Information online, Figure D), making poly-PEGDA the most desirable formulation for subsequent testing.

Burst Pressure Tests

Burst pressure measurement provided a way to evaluate the bond strength between two layers by pressurizing a liquid into the interface between them. Recent work by Dahlquist et al.⁴⁶ showed that burst pressure, and therefore bond strength, of PDMS is largely dependent on the method used to bind two layers. The burst pressure for silicon with PDMS cured without heat or adhesive is relatively weak at ~40 kPa. When PDMS curing agent is used as an adhesive and cured at room temperature, the silicon-PDMS burst pressure increases to ~130 kPa. Heat curing at 90 °C can raise the silicon-PDMS burst pressure even further to 700 kPa,⁴¹ but heat curing techniques are not compatible with protein functionalized surfaces. Pressures in the poly-PEGDA flow channel reached up to 420 kPa (Figure 2B) before the pressure sensor became disconnected from the tubing. We note that since the pressure sensor connection failed before the bonded poly-PEGDA layers, the actual burst pressure of these devices could be much higher. More accurate burst pressures for these devices could be recorded using a more robust attachment of the pressure sensor, as well as a pressure sensor with a higher pressure range. Importantly, microchannel stability to at least 420 kPa is sufficient for most applications in microfluidics.

Bulk Fluorescence Comparison

Polymers provide a simpler alternative for fabrication of microfluidics compared to glass but generally have higher background fluorescence. One of the reasons PDMS is popular is because its fluorescent background is relatively low and closer to that of glass.⁴⁷ Here, we compared the fluorescence background of PDMS and poly-PEGDA. The dark current subtracted background fluorescence signal for PDMS was ~36 CCD units. This signal was not lowered by photobleaching with 30 min of 2.3 mW/mm² 488 nm laser exposure. As-received poly-PEGDA started at a signal of 75 which dropped to ~50 after photobleaching. It is possible to further reduce the background fluorescence of poly-PEGDA by removing impurities such as inhibitors from the monomer. Poly-PEGDA made from purified monomer had a lower initial signal of ~50 CCD units, which reduced to ~35 CCD units, the same level as PDMS, after photobleaching in the same manner as the PDMS. Thus, purifying the monomer and photobleaching can make a poly-PEGDA material that offers comparable bulk background fluorescence to PDMS.

Rhodamine B Comparison

Hydrophobic molecules such as rhodamine B readily diffuse into unmodified PDMS.⁴² A comparison of the diffusion of rhodamine B in poly-PEGDA and plasma-bonded PDMS is given in Figure 3. PDMS showed a significant fluorescence signal and spatial distribution increase over 4 hr as rhodamine B diffused into the bulk PDMS surrounding the channel. In contrast, the fluorescence signal for poly-PEGDA remained confined and at levels characteristic of analyte within the channel even after 4 hr. Resistance to permeation by

small hydrophobic molecules without chemical modification demonstrates the innately superior performance of poly-PEGDA relative to PDMS.

Fluorescence Comparison

We compared nonspecific adsorption in PDMS and poly-PEGDA channels over a six order-of-magnitude range of increasing FITC-BSA concentrations (Figure 4). In this experiment, fluorescence signal can be broken down into two components: fluorescence due to FITC-BSA molecules nonspecifically bound to the top and bottom surfaces of the channel (F_s) and fluorescence from molecules in the bulk liquid in the channel (F_v). Fluorescence signals obtained from flowing FITC-BSA sample solutions contain both F_s and F_v , while signals from the PBS rinse consist of only F_s . Theoretically F_v should provide a linear increase in fluorescence with concentration resulting in a slope of 1 as long as $F_s = 0$. After only a five minute exposure to the lowest FITC-BSA concentration (1 ng/mL) and flowing at 10 μ L/min for 1 min, the background-subtracted fluorescence signal for PDMS was already higher than the detector noise level (the standard deviation of the signal prior to background subtraction). In contrast, poly-PEGDA exposed to FITC-BSA concentrations under 100 ng/mL exhibited background-subtracted fluorescence below the level of detector noise. Only at FITC-BSA concentrations above ~ 50 μ g/mL was the signal due to protein in the PDMS channel greater than the signal due to FITC-BSA nonspecifically bound to the walls ($F_v > F_s$). In contrast, the protein solution signal is distinct from F_s above ~ 10 μ g/mL FITC-BSA in poly-PEGDA, indicating lower levels of nonspecific adsorption. The slope of signal as a function of FITC-BSA concentration is well below 1 in PDMS, because of significant nonspecific adsorption at lower concentrations ($F_s \neq 0$), leading to much higher signals observed than would be expected from the channel contents alone (F_v). For just the highest two FITC-BSA concentrations (≥ 500 μ g/mL) the signal vs. concentration plot has the slope of 0.94 (~ 1) for PDMS. For poly-PEGDA exposed to FITC-BSA, the signal vs. concentration slope from 50 μ g/mL to 1 mg/mL was 0.91 (~ 1), offering an order-of-magnitude larger linear range than in PDMS. This result clearly demonstrates less nonspecific adsorption in poly-PEGDA, making our material better suited for quantitative measurements on adsorptive proteins.

Time Comparison

PDMS and poly-PEGDA behaved differently when exposed to flow of a low concentration of FITC-BSA over time (Figure 5). This experiment thus expands over a prior publication,³⁷ where only the end results of nonspecific adsorption were reported. The steady increase in fluorescence signal in the PDMS device was due to nonspecific adsorption of FITC-BSA to the channel surface in the detection window ($F_s \neq 0$). The fluorescence signal for FITC-BSA in the PDMS channel was initially less than in the poly-PEGDA channel but it slowly increased to three times the poly-PEGDA amount in 100 min. The initially lower signal in PDMS during the first ~ 20 min was most likely due to depletion of FITC-BSA flowing in the channel, through surface adsorption prior to the detection point. The PDMS signal was detected 2 mm from the sample inlet, which at the flow rate of 0.2 μ L/min gave a 14 s flow time for FITC-BSA to reach the detection point. Since only 7 s were needed for a molecule to diffuse the 40 μ m from the center of the channel to the surface, on average the introduced FITC-BSA molecules should come into contact with the wall multiple times and have an opportunity to nonspecifically bind to the surface. In contrast, the FITC-BSA signal in poly-PEGDA was detected 0.7 cm from the sample inlet, leaving ~ 50 s to reach the detection point. Even though significantly more opportunity was allowed for FITC-BSA to interact with the poly-PEGDA surface, no initial depletion zone was observed. Furthermore, the signal was essentially constant over the time of the experiment, indicating that $F_s \ll F_v$ in the detection region over time, again unlike with PDMS. Thus, it is clear that poly-PEGDA is more resistant than PDMS to surface fouling over time.

Microchip Electrophoresis

Electrophoretic separations of amino acids and proteins are shown in Figure 6. In the amino acid separation (Figure 6A) FITC-lysine eluted at 30 s and FITC-tryptophan eluted at 81 s; theoretical plate counts of 10,000 (4.0×10^5 N/m) for FITC-Lys and 4500 (1.8×10^5 N/m) for FITC-Trp were achieved. In the protein separation (Figure 6B) FITC-thyroglobulin eluted at 59 s and FITC- β -lactoglobulin A eluted at 64 s, with a resolution of 1.4. Theoretical plate numbers were 4900 (2.0×10^5 N/m) for FITC-thyroglobulin and 4400 (1.8×10^5 N/m) for FITC- β -lactoglobulin A. In comparison, Wang et al.⁴⁸ demonstrated that unmodified PDMS gave poor resolution for both amino acids and proteins. They further showed that modifying PDMS surfaces with chitosan improved the resolution, but their best theoretical plate counts were much smaller at 6.2×10^4 N/m for an amino acid and 2.2×10^4 N/m for a protein. The theoretical plate counts we show for unmodified poly-PEGDA indicate great promise for use of this material in high-performance separations.

Conclusion

A material formed from photopolymerization of poly(ethylene glycol) diacrylate was made using a similar fabrication process to PDMS. Poly-PEGDA was shown to be stable in water, have a high burst pressure (bond strength), and have optical clarity similar to PDMS. Poly-PEGDA also demonstrated excellent resistance to diffusion of small hydrophobic molecules into the bulk material, lower nonspecific binding than PDMS over a range of increasing FITC-BSA concentrations, and greater resistance over time to surface fouling during exposure to low protein concentrations. Poly-PEGDA shares with PDMS the favorable characteristic of low intrinsic fluorescent background. Finally, symmetric peaks and theoretical plate counts in electrophoretic separations of amino acids and proteins demonstrate the value of poly-PEGDA for biological sample analysis.

Low nonspecific adsorption, coupled with low background fluorescence for poly-PEGDA, makes this polymer worthy of consideration as an alternative to PDMS for microfluidic devices. An important feature of PDMS is its elasticity, which allows for the implementation of valves and pumps into microsystems. Our poly-PEGDA layers similarly have some elasticity, as demonstrated by the ability to flex or bend without breaking. Further optimization of poly-PEGDA formulations is ongoing to provide comparable mechanical properties to PDMS. Creating flexible valves and pumps entirely from poly-PEGDA would allow fewer areas for analyte adsorption and contribute to lower detection limits. The integration of nonadsorptive microfluidic materials, such as poly-PEGDA, with analyte sensing mechanisms like microcantilevers or nanowires should provide broader application and further enable the evaluation of new detection modalities in biomedical research.

Supplementary Material

Refer to Web version on PubMed Central for supplementary material.

Acknowledgments

This work was supported by the National Institutes of Health (R01 EB006124). G. Nordin was supported in part by NSF grants ECS-0602261 and IIS-0641973, and DARPA grant 66001-04-8933. This work was also supported by contracts 75523 and HHM402-8-0151 from the Pacific Northwest National Laboratory and the National Consortium for MASINT Research, respectively. Microfabrication work was carried out in the Brigham Young University Integrated Microfabrication Laboratory.

References

1. Reyes DR, Iossifidis D, Auroux P-A, Manz A. *Anal. Chem.* 2002; 74:2623–2636. [PubMed: 12090653]
2. Arora A, Simone G, Salieb-Beugelaar GB, Kim JT, Manz A. *Anal. Chem.* 2010; 82:4830–4847. [PubMed: 20462185]
3. Wang J, Ren L, Li L, Liu W, Zhou J, Yu W, Tong D, Chen S. *Lab Chip.* 2009; 9:644–652. [PubMed: 19224012]
4. Lindström S, Andersson-Svahn H. *Lab Chip.* 2010; 10:3363–3372. [PubMed: 20967379]
5. Anglin EJ, Salisbury C, Bailey S, Hor M, Macardle P, Fenech M, Thissen H, Voelcker NH. *Lab Chip.* 2010; 10:3413–3421. [PubMed: 20941408]
6. Dudek MM, Kent N, Gustafsson KM, Lindahl TL, Killard AJ. *Anal. Chem.* 2010; 83:319–328. [PubMed: 21121686]
7. Teh S-Y, Lin R, Hung L-H, Lee AP. *Lab Chip.* 2008; 8:198–220. [PubMed: 18231657]
8. Pei J, Nie J, Kennedy RT. *Anal. Chem.* 2010; 82:9261–9267. [PubMed: 20949899]
9. Huebner A, Bratton D, Whyte G, Yang M, deMello AJ, Abell C, Hollfelder F. *Lab Chip.* 2009; 9:692–698. [PubMed: 19224019]
10. Jeffries GDM, Lorenz RM, Chiu DT. *Anal. Chem.* 2010; 82:9948–9954. [PubMed: 21062029]
11. Benhabib M, Chiesl TN, Stockton AM, Scherer JR, Mathies RA. *Anal. Chem.* 2010; 82:2372–2379. [PubMed: 20151682]
12. Bruzewicz DA, Reches M, Whitesides GM. *Anal. Chem.* 2008; 80:3387–3392. [PubMed: 18333627]
13. Mellors JS, Jorabchi K, Smith LM, Ramsey JM. *Anal. Chem.* 2010; 82:967–973. [PubMed: 20058879]
14. Goral VN, Hsieh Y-C, Petzold ON, Clark JS, Yuen PK, Faris RA. *Lab Chip.* 2010; 10:3380–3386. [PubMed: 21060907]
15. Shi W, Wen H, Lu Y, Shi Y, Lin B, Qin J. *Lab Chip.* 2010; 10:2855–2863. [PubMed: 20882233]
16. Yang W, Sun X, Wang H-Y, Woolley AT. *Anal. Chem.* 2009; 81:8230–8235. [PubMed: 19728735]
17. Yang W, Yu M, Sun X, Woolley AT. *Lab Chip.* 2010; 10:2527–2533. [PubMed: 20664867]
18. Sia SK, Whitesides GM. *Electrophoresis.* 2003; 24:3563–3576. [PubMed: 14613181]
19. Huang B, Wu H, Kim S, Zare RN. *Lab Chip.* 2005; 5:1005–1007. [PubMed: 16175253]
20. Phillips KS, Kang KM, Licata L, Allbritton NL. *Lab Chip.* 2010; 10:864–870. [PubMed: 20300673]
21. Roman GT, Culbertson CT. *Langmuir.* 2006; 22:4445–4451. [PubMed: 16618201]
22. Séguin C, McLachlan JM, Norton PR, Lagugné-Labarthe F. *Appl. Surf. Sci.* 2010; 256:2524–2531.
23. Barbier V, Tatoulian M, Li H, Arefi-Khonsari F, Ajdari A, Tabeling P. *Langmuir.* 2006; 22:5230–5232. [PubMed: 16732644]
24. Kim B-Y, Hong L-Y, Chung Y-M, Kim D-P, Lee C-S. *Adv. Funct. Mater.* 2009; 19:3796–3803.
25. Bodas D, Khan-Malek C. *Microelectron. Eng.* 2006; 83:1277–1279.
26. Hillborg H, Tomczak N, Oláh A, Schönherr H, Vancso GJ. *Langmuir.* 2004; 20:785–794. [PubMed: 15773106]
27. Bausch GG, Stasser JL, Tonge JS, Owen MJ. *Plasmas Polymers.* 1998; 3:23–34.
28. Wang D, Oleschuk RD, Horton JH. *Langmuir.* 2008; 24:1080–1086. [PubMed: 18163653]
29. Sui G, Wang J, Lee C-C, Lu W, Lee SP, Leyton JV, Wu AM, Tseng HR. *Anal. Chem.* 2006; 78:5543–5551. [PubMed: 16878894]
30. Truong TT, Lin R, Jeon S, Lee HH, Maria J, Gaur A, Hua F, Meinel I, Rogers JA. *Langmuir.* 2007; 23:2898–2905. [PubMed: 17261048]
31. Willis PA, Greer F, Lee MC, Smith JA, White VE, Grunthaner FJ, Sprague JJ, Rolland JP. *Lab Chip.* 2008; 8:1024–1026. [PubMed: 18584073]

32. Fiorini GS, Lorenz RM, Kuo JS, Chiu DT. *Anal. Chem.* 2004; 76:4697–4704. [PubMed: 15307779]
33. Pan T, Fiorini GS, Chiu DT, Woolley AT. *Electrophoresis.* 2007; 28:2904–2911. [PubMed: 17640094]
34. Schlapak R, Pammer P, Armitage D, Zhu R, Hinterdorfer P, Vaupel M, Frühwirth T, Howorka S. *Langmuir.* 2006; 22:277–285. [PubMed: 16378432]
35. Klasner SA, Metto EC, Roman GT, Culbertson CT. *Langmuir.* 2009; 25:10390–10396. [PubMed: 19572528]
36. Liu JK, Sun XF, Lee ML. *Anal. Chem.* 2007; 79:1926–1931. [PubMed: 17249641]
37. Kim P, Jeong HE, Khademhosseini A, Suh KY. *Lab Chip.* 2006; 6:1432–1437. [PubMed: 17066166]
38. Duffy DC, McDonald JC, Schueller OJA, Whitesides GM. *Anal. Chem.* 1998; 70:4974–4984. [PubMed: 21644679]
39. Cooksey GA, Elliott JT, Plant AL. *Anal. Chem.* 2011; 83:3890–3896. [PubMed: 21506521]
40. Afshar R, Moser Y, Lehnert T, Gijss MAM. *Anal. Chem.* 2011; 83:1022–1029. [PubMed: 21214193]
41. Satyanarayana S, Karnik RN, Majumdar A. *J. Microelectromech. Syst.* 2005; 14:392–399.
42. Roman GT, Hlaus T, Bass KJ, Seelhammer TG, Culbertson CT. *Anal. Chem.* 2005; 77:1414–1422. [PubMed: 15732926]
43. Berthier, J.; Silberzan, P. *Microfluidics for Biotechnology.* Norwood: Artech House; 2006. p. 95
44. Placidi M, Cannistraro S. *Europhys. Lett.* 1998; 43:476–481.
45. Kelly RT, Woolley AT. *Anal. Chem.* 2003; 75:1941–1945. [PubMed: 12713054]
46. Dahlquist WC, Kim S, Nordin GP. Room Temperature Bonding of Polydimethylsiloxane (PDMS) Microfluidics to Silicon-Based Sensors. *J. Micro/Nanolithogr., MEMS MOEMS.* 2011 submitted for publication.
47. Pai J-H, Wang Y, Salazar GT, Sims CE, Bachman M, Li GP, Allbritton NL. *Anal. Chem.* 2007; 79:8774–8780. [PubMed: 17949059]
48. Wang A-J, Xu J-J, Chen H-Y. *J. Chromatogr., A.* 2007; 1147:120–126. [PubMed: 17320888]

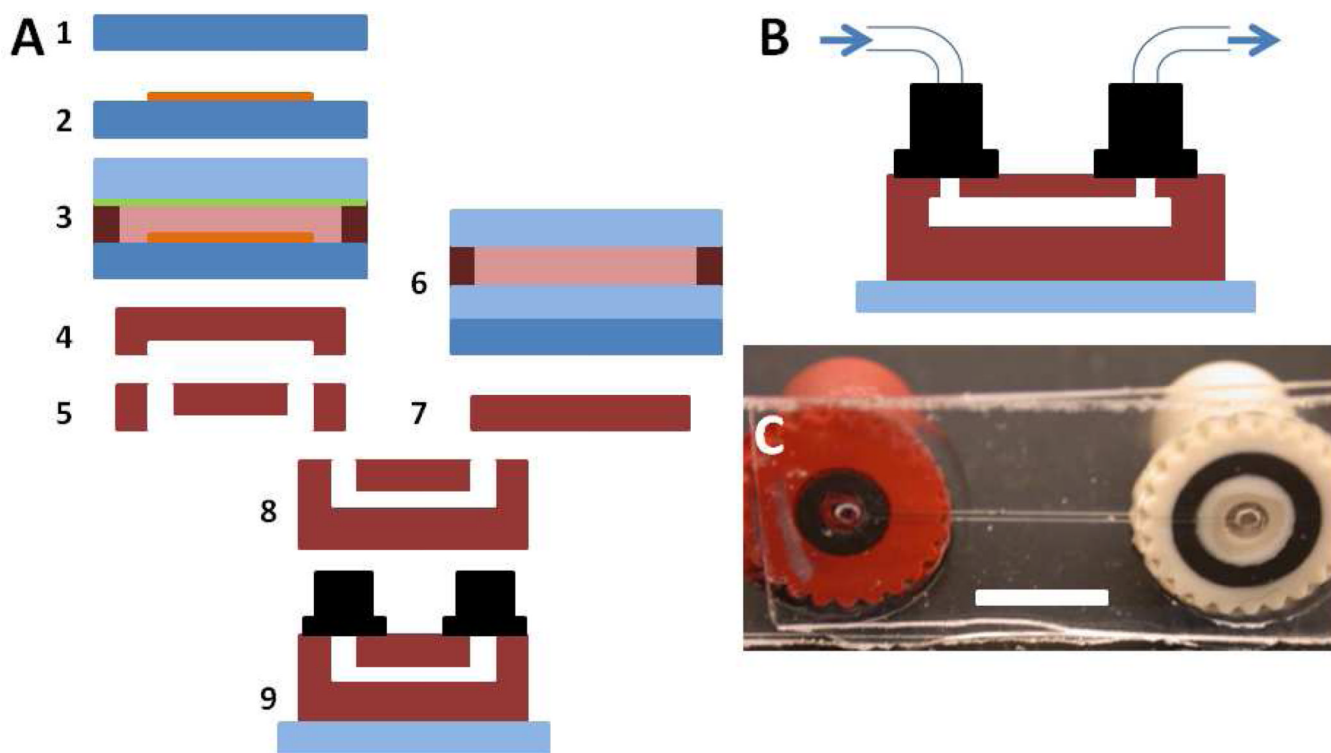


Figure 1. Poly-PEGDA flow channel device used to evaluate nonspecific adsorption

(A) Fabrication process for making a flow channel in poly-PEGDA. Polymerized PEGDA layers and spacers are shown in red, unpolymerized PEGDA in pink, SU8 in orange, PDMS in green, silicon wafer in dark blue, and glass wafer in light blue. (1–2) Patterning of SU8 photoresist is the same as in Figure 1A-1, 2. (3) PEGDA is polymerized. (4) Polymerized PEGDA is removed. (5) Holes are cut in poly-PEGDA using a CO₂ laser. (6) An unpatterned layer of PEGDA is polymerized. (7) Poly-PEGDA is removed. (8) Poly-PEGDA layers are bonded. (9) Nanoport connectors are attached and the complete device is affixed to a glass slide. See text for further details. (B) Side-view schematic of a poly-PEGDA device. Channel is 1.5–2.5 cm long, 60–80 μm high, and 300 μm wide. Top and bottom layers are ~ 350 μm thick. (C) Bottom-view photograph of a finished poly-PEGDA device; white bar is 0.5 cm.

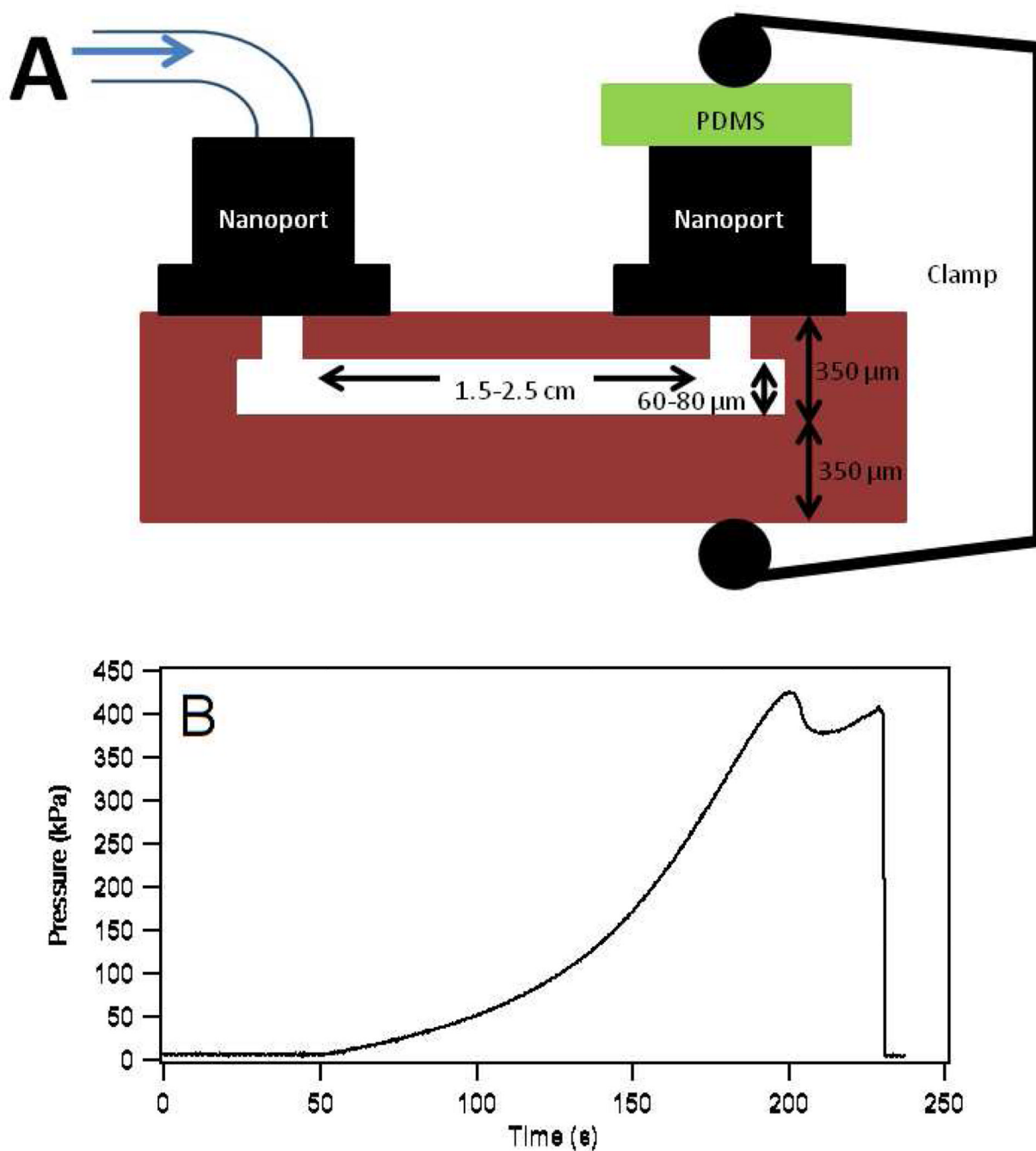


Figure 2. Burst pressure testing of bond strength between poly-PEGDA layers

(A) Side-view schematic of the poly-PEGDA device setup for burst pressure tests. Water is introduced into the channel and the channel is sealed using a piece of PDMS held in place with a clamp while pressure is applied. (B) Graph of pressure build up in a poly-PEGDA flow channel made using 0.0015% DMPA photoinitiator. Pressure release due to failure of some attachment point (in this case, the pressure gauge connection) is seen as the sudden drop at ~230 s. Since the poly-PEGDA did not delaminate, the burst pressure was at least 420 kPa.

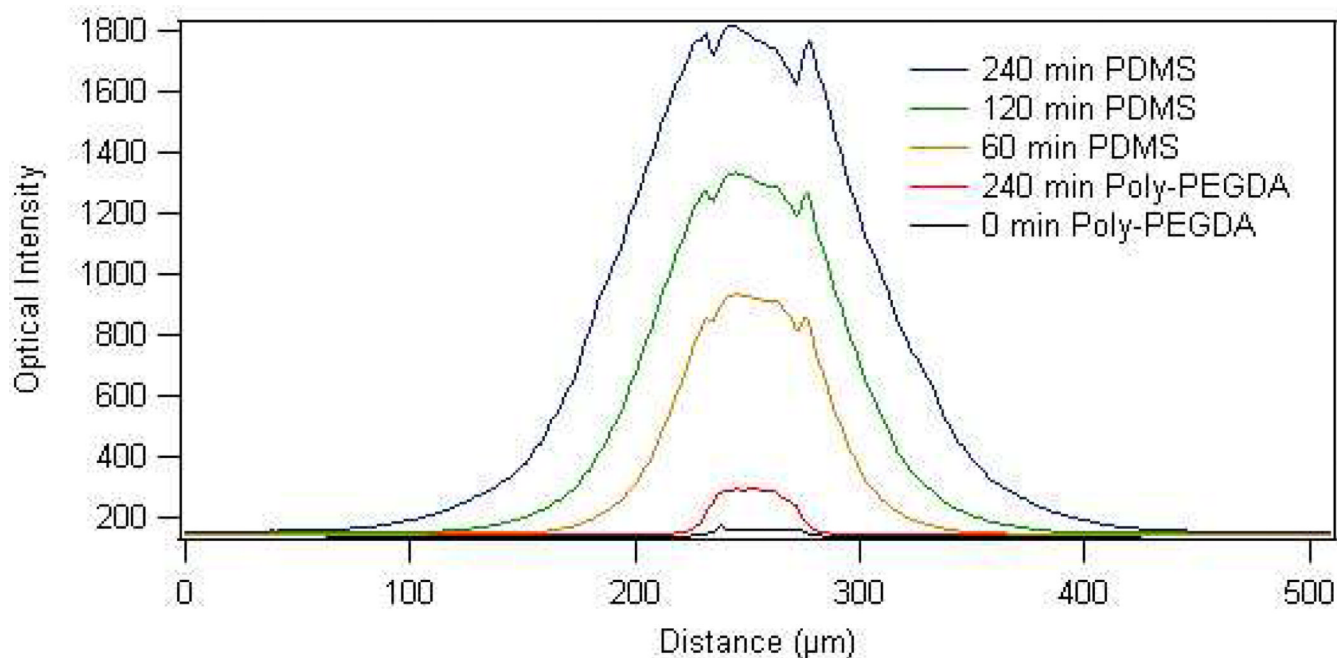


Figure 3. Plot of fluorescence signal cross sections at different times during flow of 10 μM rhodamine B at 0.2 $\mu\text{L}/\text{min}$ in 50 μm wide channels in poly-PEGDA and plasma-bonded PDMS Fluorescence in PDMS increases as rhodamine B diffuses into the polymer over 4 hr, indicating susceptibility to permeation by hydrophobic molecules. After 4 hr of exposure to rhodamine B, fluorescence signal in poly-PEGDA remains confined to the channel. Initial background buffer signal (0 min) before analyte flow was comparable for PDMS and poly-PEGDA, so only the result for poly-PEGDA is shown.

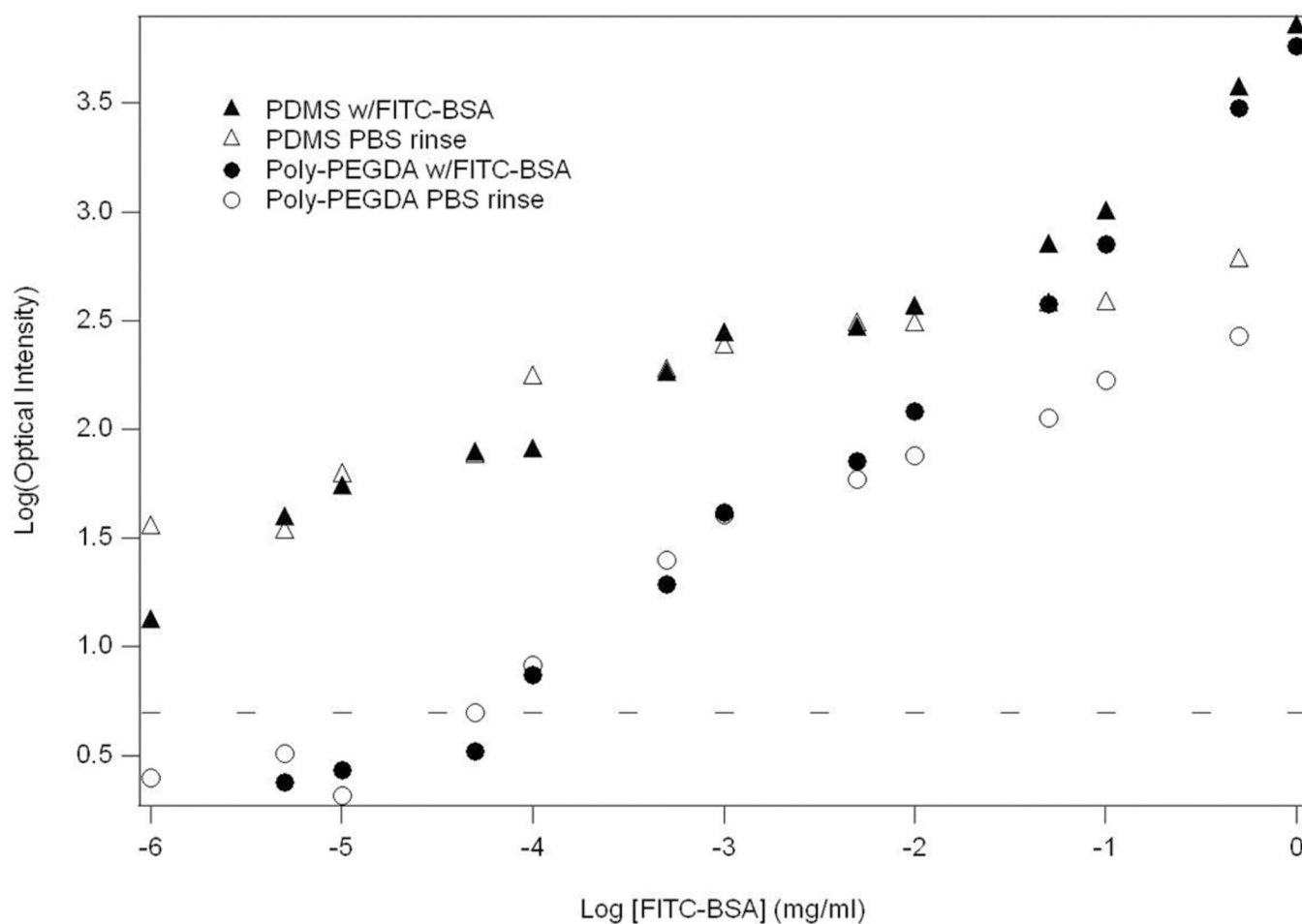


Figure 4. Background-subtracted fluorescence signal in PDMS and poly-PEGDA microdevices for increasing FITC-BSA concentrations

Solid shapes are signals from when FITC-BSA solution was in the channel. Hollow shapes are signals during a PBS rinse. The detector noise level (the standard deviation of the signal before background subtraction) is shown as a dashed line. In poly-PEGDA the signal for 1 ng/mL FITC-BSA was at the level of dark current and was not plotted.

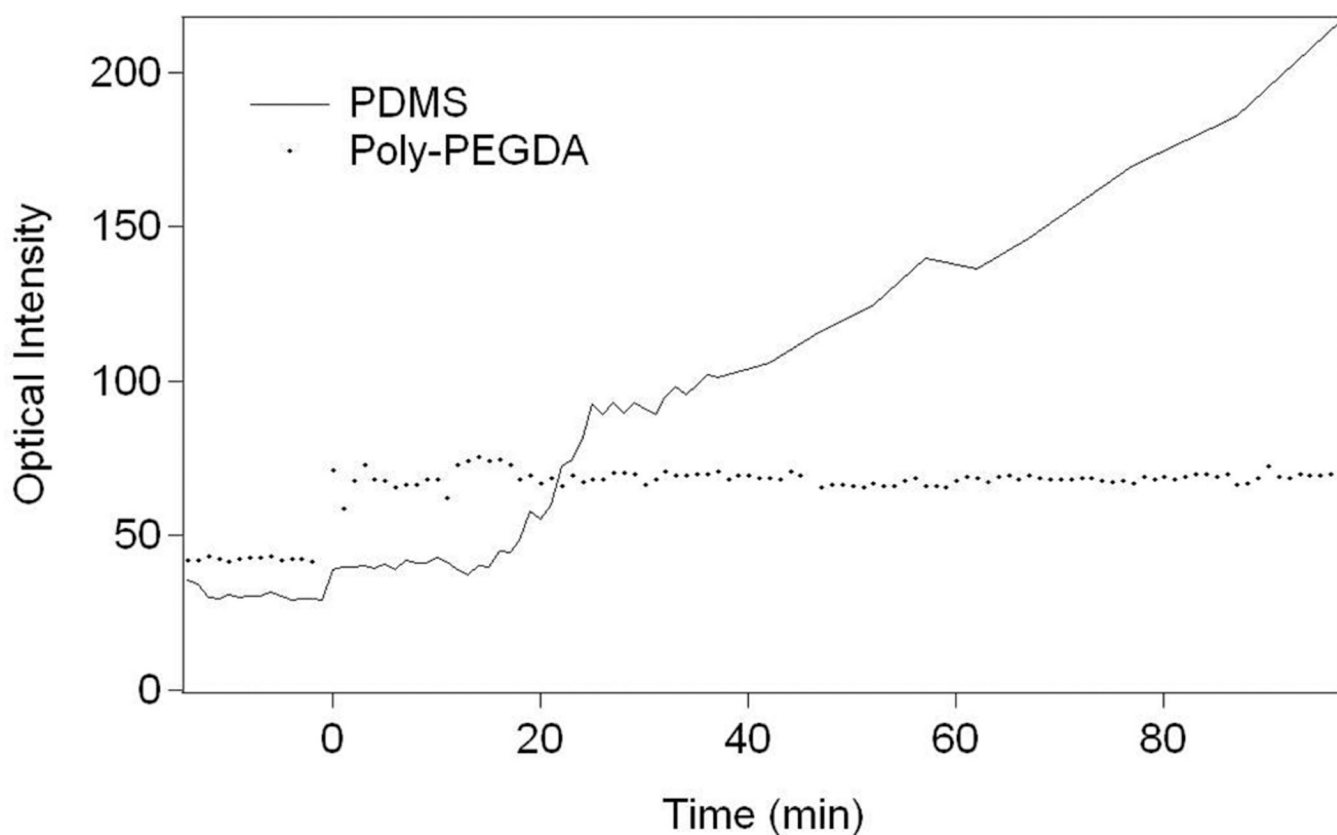


Figure 5. Fluorescence comparison of PDMS and poly-PEGDA over time during flow of a dilute FITC-BSA solution

A 1 $\mu\text{g/mL}$ solution of FITC-BSA was flowed at 0.2 $\mu\text{L/min}$. The signal in PDMS increased substantially while that in poly-PEGDA remained stable. Signal is dark current subtracted. The laser was shuttered between each fluorescence image to avoid photobleaching in the detection zone.

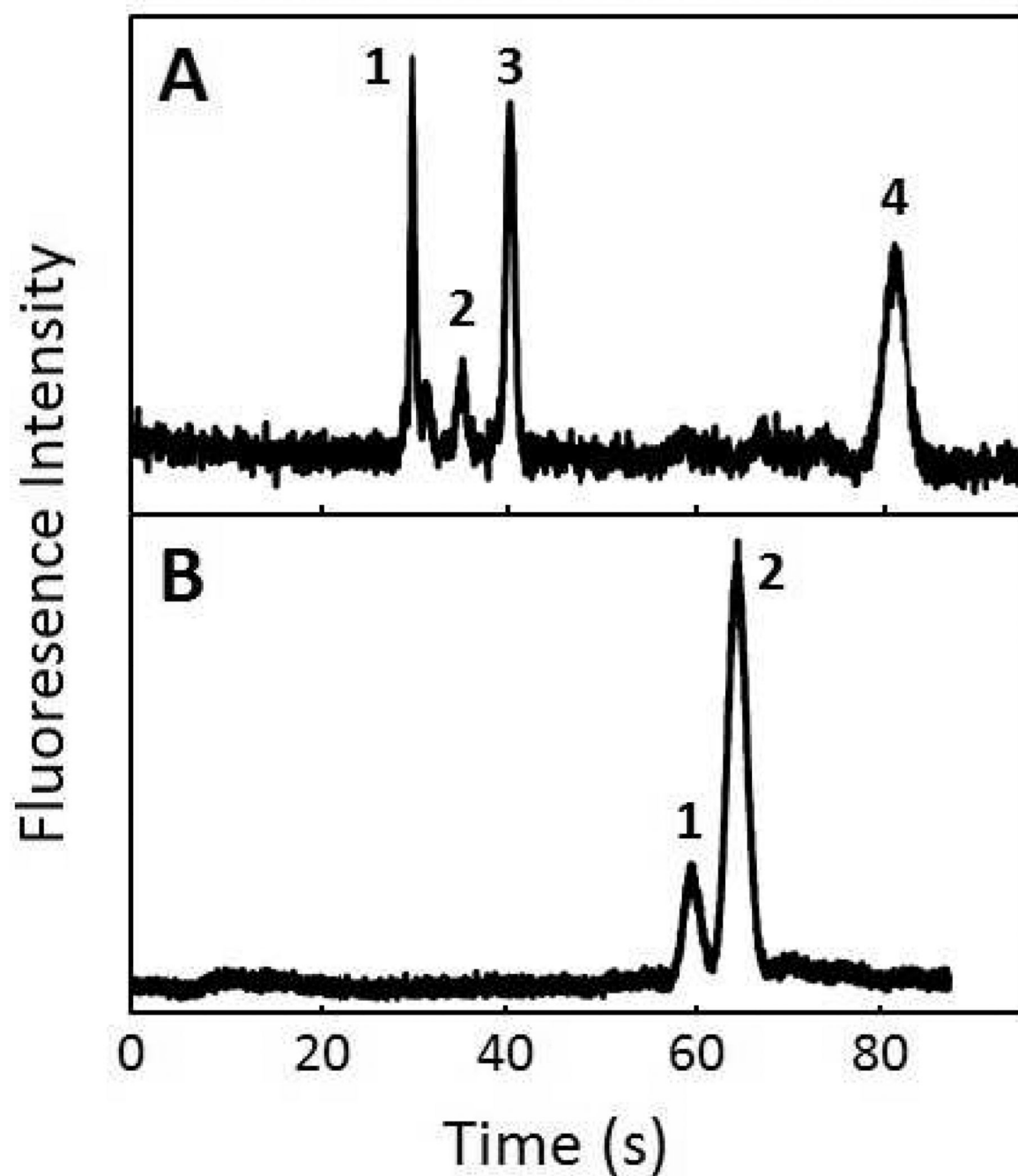


Figure 6. Electrophoretic separation of amino acids and proteins using a poly-PEGDA Microchip

(A) Separation of 1 μ M FITC-Lys (1) and 1 μ M FITC-Trp (4). Peaks 2 and 3 due to free FITC are well separated from the labeled amino acids. (B) Separation of 1 μ g/mL FITC-thyroglobulin (1) and 10 μ g/mL FITC- β -lactoglobulin A (2).